Novel role of substance-p as a systemic wound messenger to mobilize mesenchymal stem cell from bone marrow and be engaged in the wound healing epithelial layer

Hyun Sook Hong[1], Jung Sun Lee[2], Young Sam Kwon[3], Eun Kyung Lee[1], Woosung Ahn[1], Jae Chan Kim[3*], and Youngsook Son[1]*

[1]Graduate School of Biotechnology & College of Life Science, Kyung Hee University, Yong In, [2]R&D Institute, McTT, Seoul, and [3]Department of Ophthalmology, College of Medicine, Chung-Ang University, Seoul, Korea,

Keywords: Substance-p, mesenchymal stem cell, transdifferentiation, mobilization, β-catenin, wound healing

Running title; SP stimulated mobilization of mesenchymal stem cell and wound healing

*Primary correspondence to:
Youngsook Son Ph.D.
Graduate School of Biotechnology & College of Life Science, Kyung Hee University, Seochun-dong, Kiheung-ku, Yong In, 441-706,Korea
Tel : 82-31-201-3822, Fax : 82-31-206-3829
E-mail : ysson@khu.ac.kr
For clinical implication
Jae Chan Kim M.D., Ph.D.
Dept. of Ophthalmology, College of Medicine, Chung-Ang University, Seoul 140-757, Korea
Tel : 82-2-748-9838 Fax : 82-2-792-6295
Email:jck50ey@kornet.net

Abstract

Tissue injury may bring up the systemic participation of bone marrow stem cells in the repair. In this study, we report that substance-p is a systemically acting messenger to mobilize mesenchymal stem cell (MSC) probably from the bone marrow and be engaged in the wound healing process. This was supported by the injury-inducible substance-p detection in the tissue and the peripheral blood and subsequent MSC mobilization in the alkali-burn rabbit eye model, whose kinetics were dependent on the wound size. Furthermore, i.v. injection of exogenous substance-p stimulated MSC mobilization in the uninjured rabbits and those mobilized cells showed multipotent differentiation capacity. We demonstrated that earlier substance-p elevation in the circulation by substance-p injection or transfusion of autologous PKH-labeled MSC mobilized by substance-p strongly accelerated the wound healing of the alkali-burned rabbit eye and the transfused MSCs were engrafted to the epithelial and stromal layer of the injured tissue, suggesting their epithelial transdifferentiation in the regenerating tissue. Finally, we showed that substance-p stimulated transmigration of human MSC with concomitant induction of MMPs and inhibition of their inhibitors, cell proliferation, ERK1/2 activation, and nuclear translocation of β-catenin in vitro. In conclusion, substance-p plays a role as a systemic wound-messenger to promote the MSC mobilization from the marrow and their participation in the wound healing possibly through its stimulant effect on MSC repopulation as well.

Introduction

Tissue injury may create a unique and specific wound microenvironment composed of cytokines, chemokines, growth factors, and neurohormones, which are released from the surrounding epithelium, stroma, sensory neuron, and peripheral blood due to the injury (1, 2). Some of them are known to activate inflammatory response. Others, yet to be identified, may play roles as injury-specific endogenous factors, which can be sensed by the bone marrow (BM) cells or neighboring cells that in turn stimulate their migration to the damaged tissue and promote structural and functional repair.

Many previous reports strongly suggest that BM-derived cells, either by endogenous mobilization or transfusion, are actively involved in the repair of tissue injury such as myocardiac infarction (MI) (3-6), lung injury (7, 8), skin wound (9-11), and liver injury (12). Mainly, it was explored in the context of intravenous supply of exogenous G-CSF or GM-CSF to stimulate circulatory mobilization of endothelial precursor cells (EPC) (13), HSC (14), and MSC in the ischemic MI, and stromal cell-derived factor-1 (SDF-1) dependent EPC homing to the injured tissue (15, 16). In the bleomycin-induced lung injury, transfused BM-MSC was shown to be transdifferentiated into specific and distinct lung cell phenotypes (8). Thus BM-MSC has been already anticipated for their homing to the injured site and subsequent tissue-specific transdifferentiation.

Even though BM-MSC was highly anticipated not only in the mesenchyme tissue repair but also in other epithelial or neural tissue, endogenous factors specific for their mobilization from the BM and homing to the injured site have not been reported yet. However, recent reports such that MSC or MSC like cells are frequently detected in tissues other than the BM such as fat tissue (17), wound healing tissue (18, 19), and pterygium (20), strongly suggest the existence of certain endogenous factors governing MSC trafficking from the BM to the peripheral tissue. Those factors may be transiently stimulated during the period of the tissue injury and repair or under the certain patho-physiological condition.

Substance-p (SP) is an 11 amino acid neuropeptide encoded by the preprotachykinin-1 (PPT-1) gene and has the same peptide sequence among the mouse, the rabbit, and the human (NCBI access #M68909, X62994 and

NM013998 respectively). SP preferentially binds to NK-1 receptor (NK-1R) and activates G-protein-linked signaling pathway and MAPK/ERK pathway in the spiral ganglion neuron, smooth muscle cells, and glioma cells (21-23), leading to its cell proliferating effect. Diversity of SP expression in neural system as well as in non-neural tissue such as BM stromal cells (24), epithelial cells (25), endothelial cells, macrophages (26), neutrophiles, and tumor cells (27) leads us to predict more extended roles of SP, aside from its pain transmitting neurotransmitter, such as neuroimmune modulation (28), the BM fibrosis (29), the tumor cell proliferation (21, 22), and the cutaneous wound healing (30-33). The SP's positive role in the wound healing within the local microenvironment was proposed by direct innervation of SP-nerve ending in the skin (34) and cornea (35) and SP-stimulated alleviation of the delayed healing under the trigeminal denervation in the eye as well as in the Capsaicin-induced neurotrophic keratopathy (36). However the systemic effect of SP has not yet been explored in the context with MSC mobilization and their recruitment in the injured tissue.

In this study, we report that SP was an early injury-inductive factor detected in the injured tissue and subsequently in the peripheral blood (PB) after the alkali burn injury on the mouse and rabbit eye and its induction kinetic in the circulation was dependent on the wound size. In order to address the SP's role as a systemic wound messenger to mobilize MSC, this function of SP was injury-independently proved by i.v. injection of exogenous SP and subsequent MSC mobilization in uninjured mice as well as rabbits. Furthermore, SP's stimulatory role in the wound healing in accordance with its role in the MSC mobilizer from the BM was independently proven based on the accelerated wound recovery from the alkali-burn on the rabbit eye either by SP i.v. injection just after the injury or by autologous transplantation of SP-dependently mobilized MSC (MSC^{sp}). In addition, SP's mechanism on the MSC mobilization and MSC repopulation in the BM was further explored in the human MSC.

Results

SP as an early injury-inducible factor detected in the injured tissue and in the circulation

Injury-inducible factors in the injured tissue were analyzed in the alkali-burned murine eyes by RT-PCR analysis (**Fig. 1a**). SP, IL-1, TNF-α, hypoxia-inducible factor 1α (HIF-1α) and VEGFR1 were expressed in the injured eye from 1 day, SCF and Placental growth factor (PIGF) from 3 day, and VEGFR2 from 14 day. For systemic analysis of their inductions, ELISA was carried out in the PB sample (**Fig. 1b**). Among the early injury-inducible factors detected in the injured eye, the SP peptide was increased 3.2 folds in the PB on 1 day, 4.4 folds on 3 day, and 1.3 folds on 5 day, comparing to the uninjured control. IL-1 and TNF-α, inflammatory cytokines, were also elevated but later and smaller than those of SP. By immunohistochemical staining with SP Ab, CD29 Ab, and α–SMA Ab, SP peptide was strongly detected in the early injured tissue on 1 day but disappeared mostly on 3 day, suggesting its earlier regression in the injured tissue than the termination of the inflammatory phase (**Supplementary Fig. 1a** online). In the fibroplasia phase of injured tissue, actively migrating large $CD29^+$ and $\alpha\text{-SMA}^+$ fibroblastic cells were detected among inflammatory cells (**Supplementary Fig. 1b** online).

SP-specific mobilization of $CD29^+$ fibroblastic cells into the PB of the uninjured mice, possibly from the bone marrow

From the data such as the injury-inducible SP increase in the PB and transient detection of $CD29^+$, $\alpha\text{-SMA}^+$ fibroblastic cells in the injured tissue, we hypothesized that SP may bring up systemic effect on the BM, probably by mobilizing MSC into the PB and then their recruitment to the wound site. In order to investigate this role of SP independently from other injury-inducible factors, the 11 amino acid SP peptide was i.v. injected in the uninjured mice at a dose of 5.0 nmole/kg, which approximately corresponds to the 100nM after dilution in total

blood. Then the $CD29^+$ attached cells, distinguished from the $CD29^-$, $CD45^+$ macrophages among the attached PB mononuclear cells, were monitored (**Fig. 1c**, **Supplementary Fig. 2 a, b** online). Exogenous SP injection stimulated $CD29^+$ cell mobilization in the PB approximately fifteen folds 1 day and ten folds 2 day comparing to the PBS-injected group, which was blocked by concomitant injection of mouse specific NK-1R, blocker, R67850. Initially round-shaped and attached $CD29^+$ cells, specifically mobilized by SP injection, turned into fibroblastic morphology within 3-5 day culture and all those fibroblastic cells were $CD29^+$, $CD117^+$, $CD166^+$, α-SMA^+, $CD34^-$, and $CD45^-$ based on immunofluorescence staining (**Supplementary Fig. 2c** online), probably corresponding to MSC. This result strongly suggests a yet unidentified role of SP as a MSC mobilizer.

Then, alkaline phosphatase (AP)-conjugated SP peptide was i.v. injected to explore the tissue origin of the mobilized $CD29^+$ cells and then AP activity was measured in the attached cells of the BM flush (**Fig.1 d**). Strong AP activity was detected among live attached cell clusters of the BM flush at 2 h and 4 h post injection, which corresponded to the $CD29^+$ cell clusters based on subsequent immunocytochemical staining with CD29 Ab after the cell fixation (**Fig. 1e**). The AP activity detected in the BM flush was contributed by AP-conjugated SP bound to the $CD29^+$ cell clusters in the BM flush since SP treatment to cultured human MSC did not stimulate any AP activity (**Supplementary Fig. 3** online). Thus, the i.v. injected SP reached to the BM and bound to the $CD29^+$ cells at least within 2 h post injection even though the $CD29^+$ cell mobilization was obvious at 1 day post injection in the mouse.

Correlation of the wound-size with SP induction kinetics and subsequent $CD29^+$ cell mobilization

If the injury-inducible SP rise in the PB plays a role as a wound messenger, the larger wound may induce the more and the faster SP rise in the PB. In order to test this hypothesis, rabbits were alkali-burned either on one site per eye (two wounds per rabbit, n= 5 per group) or two sites per eye (four wounds per rabbit, n= 5 per group) and the SP level in the PB of the same rabbit was sequentially monitored up to 72 h post burn (**Fig. 2a, b**). In contrast to the gradual SP elevation in the PB of one wound per eye, two wounds per eye showed maximal level of SP

induction even at 1 h post burn, whose level sustained up to 3 day observation period. Thus if the bigger the injury was made, the earlier and higher SP induction in the PB was achieved.

Effect of the wound size-dependent SP rise on the $CD29^+$ MSC mobilization kinetic was examined by measuring initial time and magnitude of $CD29^+$ cell mobilization in the PB from the 10 ml PB of the same rabbit sequentially, 3 day, 5 day, and 7 day post burn (**Fig. 2c**). In all the five rabbits with one wound per eye, no $CD29^+$ cell was detected in the PB until 5 day post burn but its mobilization became obvious 7 day post burn (**Fig. 2c**) and got bigger 9 day post burn (**Fig. 3e**). However, in all the five rabbits with two wounds per eye (total four wounds per rabbit), the $CD29^+$ cell mobilization was clearly observed on 5 day, sustained up to 7 day (**Fig. 2c**), and got attenuated 9 day post burn (data not shown). Among them, four rabbits except one showed higher $CD29^+$ cell mobilization on 5 day than 7 day post burn. Thus the SP induction kinetic (time for maximal induction and duration) is determined by the wound-size (**Fig. 2b**), which in turn positively affects the start time and possibly the magnitude of the $CD29^+$ cell mobilization with the 4-5 days lag after maximal SP peak in the PB.

Characterization of $CD29^+$ cells in the PB mobilized by SP injection

SP injection in the uninjured rabbit, similarly to the mouse data (**Fig. 1**), was sufficient enough to mobilize $CD29^+$ cells in the PB at least within 3 days without stimulation of $CD29^-$ $CD45^+$ macrophage mobilization (**Fig. 2d**), approximately 80 folds than in the PBS-injected rabbits (**Fig. 2e**). In contrast, HSC-CFU in the PB was stimulated approximately 2 folds (**Fig. 2f**). After 4 week culture, all the $CD29^+$ attached cells expressed keratin 3 (K3), CD29, and α-SMA (**Fig. 2g, h**). Unexpectedly, SP-dependently mobilized $CD29^+$, $CD45^-$, α-SMA^+ fibroblastic cells expressed K3, previously known to be a corneal epithelial specific marker, whose expression was also confirmed in the $Stro\text{-}1^+$ human MSC (**Supplementary Fig. 4** online). The K3-expressing $CD29^+$, $CD45^-$, α-SMA^+ fibroblastic cells could be differentiated into adipocytes based on the oil red-O staining, into osteoblasts based on the alkaline phosphatase activity, into chondrocytes based on the lacunae formation and Safranin-O staining (**Fig. 2i**). Based on their multi-potent differentiation capacity as well as their distinct profiles of cell surface markers, the $CD29^+$, $CD45^-$, α-SMA^+, $K3^+$ fibroblastic cells mobilized by the SP injection were

probably multi-potent MSCs, noted as MSC^{sp} in this text in order to distinguish MSC (MSC^{BM}) derived from the BM.

Accelerated wound healing along with earlier MSC^{sp} mobilization by SP i.v. injection after the alkali-burn

To further determine the SP's role as a systemic wound messenger positively working on the tissue repair, SP was i.v. injected just after and 1 day post burn in the rabbit with one wound per eye which showed gradual reach SP peak in the PB, approximately 3 day post burn (**Fig. 2b**). SP injections markedly accelerated the burn recovery as judged by the regain of the surface transparency and the disappearance of hemorrhagic regions in the limbus and conjunctiva (**Fig. 3a**) and by the histological observations showing full thickness coverage of epithelium, well organized vasculature, and ordered array of dense collagen bundles, which were closely resembled with those of collateral unburned side of the same eyes except the still presence of macrophages and polymorphonuclear giant cells just beneath the limbal epithelium, comparing to the PBS-injected burn control (**Fig. 3b**). In contrast, the PBS-injected burn control showed only very thin coverage of epithelium, active infiltration of large $CD29^+$ fibroblastic cells and loose unorganized collagen fibrils in the stroma, which was similar to the histological observation on 5 day in the SP injected group (data not shown). SP injection accelerated the initial time of the $CD29^+$, α-SMA^+ double positive cell mobilization at least 3-4 days earlier than in the PBS-injected burn control (**Fig. 3c**) but did not affect the $CD29^-$, $CD45^+$ macrophage mobilization (**Fig. 3d**). Multiple PB samplings from the same rabbit caused slightly delayed healing comparing to the non-withdrawn rabbit, probably due to the removal of the mobilized cells by the blood sampling (data not shown). Thus, accelerated mobilization of $CD29^+$, α-SMA^+ $CD45^-$ fibroblastic cells (MSC^{sp}) in the PB by SP injection again support that the SP is a systemic wound messenger and a wound healing stimulant by its function of MSC mobilizer.

SP-dose dependency in the start time of MSC^{sp} mobilization and the regression of HSC in the PB

SP level in the PB seems to control $CD29^+$ cell mobilization kinetic (**Fig. 2b, c** and **Fig. 3c**) and also the wound healing rate (**Fig. 3a,b**). We investigated whether SP injection doses can control MSC mobilization (**Fig. 3e, f**) as well as the wound healing rate (**Supplementary Fig. 5** online) or not. Only at the SP-dose of 5.0nmole/kg, $CD29^+$ cell mobilization started from 3 day post burn, at the 0.5nmole/kg and 0.05nmole/kg from 5 day, and from 7 day in PBS-injected burn control (**Fig. 3e**) and all of those mobilized cells in the PB, even though their mobilization time is different, were $CD29^+$, α-SMA^+, $K3^+$ MSC^{sp} based on RT-PCR analysis (**Fig. 3f**).

SP itself seems to retain only minimal effect on the HSC mobilization comparing to marked stimulation in the MSC^{sp} mobilization of uninjured rabbit (**Fig. 2f**). However SP may indirectly affect HSC mobilization provoked by the tissue injury and subsequent inflammation by accelerating MSC^{sp} mobilization and the wound healing rate. We examined whether SP injection can affect the injury-stimulated HSC mobilization kinetic or not (**Fig. 3g**). In the burn control (SP 0.0nmole/kg), HSC-CFU in the PB was highest at 5 day and regressed at 7 day, corresponding to the start time of MSC mobilization. In the SP injected group, kinetic of HSC-CFU in the PB was forwardly shifted, steeply regressed close to the basal level on 5 day at SP 5.0nmole/kg, and gradually decayed over the time at SP 0.5nmole/kg and 0.05nmole/kg. Thus HCS-CFU decay time was affected by the MSC^{sp} mobilization time, possibly resulting in the accelerated wound healing rate and premature termination of inflammatory phase.

Accelerated wound healing by autologous MSC^{sp} transfusion and their epithelial localization in the injured tissue

The mobilized MSC^{sp} is expected to participate in the regeneration of the injured tissue. In order to demonstrate the engagement of MSC^{sp} in the tissue repair, cultured autologous PKH-labeled $MSCs^{sp}$ ($5X10^6$ cells) were transfused to the alkali-burned rabbit on 3 day post burn, approximately corresponding to the start of $MSCs^{sp}$ mobilization by SP 5.0nmole/kg injection. Their engraftment to the injured tissue was examined and their effect on wound healing was compared with the SP-injected or PBS-injected burn control (**Fig. 4**). $MSCs^{sp}$ transfusion accelerated the wound healing similarly to the SP-injected group but much faster than in the PBS-injected burn control (**Fig. 4a**). Full coverage of epithelial layer,

similarly to that of the unburned side, was achieved both in the SP-injected and in the $MSCs^{sp}$ transfused rabbits, comparing to the impaired coverage of the epithelial layer of the burn control. Loosely aggregating cells apposed between the epithelial layer and the stromal layer of the limbus were frequently detected in the transfused group (**Fig. 4b**), suggesting active upward insertion of the transfused cells from the stromal region into the epithelial layer.

PKH-labeled transfused cells were brightly detected in all the epithelial layers as well as in the stroma of the regenerated tissue, depending on the degree of the healing rate (**Fig. 4c**) but no PKH-labeled cell was detected in the uninjured collateral side (**Fig. 4d**). Among the PKH-labeled cells in the tissue, those in the stroma still expressed α-SMA but those incorporated in the epithelial layer were negative in α-SMA expression (**Fig. 4c**, α-SMA panel). Thus transfused MSC^{sp} seems to lose α-SMA expression capacity after their integration in the epithelial layer. In certain region of the stroma, K3-expressing cells without PKH-labeling (**Fig. 4c**, K3 panel), probably corresponding to endogenous MSC mobilized by the injury-induced endogenous SP, were also often noted, similarly to those of the burn control (**Fig. 4e**, K3 panel). Most features in the regenerated tissue of MSC^{sp} transfused rabbits were similar to those in the SP-injected group (**Fig. 4f**). Transfusion of allogeneic MSC^{SP} or MSC^{BM} also accelerated wound healing as well as epithelial integration (**Supplementary Fig. 6, 7** online)

SP-dependent transmigration of human MSCs with concomitant induction of proteolytic enzymes

How can SP induce the migration of MSC attached on the marrow stroma? To explore the mobilization mechanism, human MSCs were plated on top of collagen gel and SP was applied to the bottom dish. SP stimulated transmigration of human MSC in a dose dependent manner (**Fig. 5a**) and along with concomitant induction of MMP-2 and MMP-9 (**Fig. 5b**). Complete migration of human MSC in the upper chamber took approximately 3 days. Then to determine whether human MSC migration is SP-specific and chemo-attractive one or not, NK-1R blocker, L732138 specific for human NK-1R, was concomitantly applied or SP-gradient was

abolished by application of the same concentrations of SP in both sides of the chamber (**Fig. 5c**). The SP-dependent transmigration of human MSC was specifically inhibited by its receptor blocker and partially blocked by abolishment of the SP-gradient.

Effect of SP on biosynthesis of MMP-1, MMP-2, MMP-9, Tissue inhibitor of MMPs (TIMP)-1, and TIMP-2 was examined in the culture medium of ^{35}S-methionine labeled human MSCs (**Fig. 5d**). Biosynthesis of MMP-1, MMP-2, and MMP-9 was stimulated by the SP but their inhibitors such as TIMP-1 and TIMP-2 were inhibited by the SP in a dose dependent manner.

Membrane type-1 matrix metalloproteinase (MT1-MMP) is known to make the activation-processing trimeric complex with TIMP-2 and MMP-2 for the activation-cleavage of proMMP-2 (38), which was also elevated by the SP in a dose dependent manner based on the western blot (**Fig. 5e**) and immunofluorescence staining (**Fig. 5f**). In the immunoprecipitation of the cell lysate, the cell-associated TIMP-2 was not reduced by SP treatment even though their detection in the supernatant was decreased and the cell-associated MMP-2 was increased by the SP treatment, suggesting trimeric activation cleavage complex with MT1-MMP. Thus, SP stimulated human MSC to shift the proteolytic balance favorable for the collagen degradation by increasing matrix degrading molecules and concomitantly decreasing their inhibitors, which in turn makes a favorable environment for MSC mobilization.

SP-stimulated cell proliferation, ERK1/2 activation, and nuclear translocation of β-catenin in human MSC

If SP retains only the capacity of MSC mobilization from the BM, the BM stroma may become empty in the MSC pool after their mobilization. Thus, the SP effect was examined in the cultured human MSC at the aspect of cell proliferation and self–renewal capacity (**Fig. 6**). SP increased the number of viable cells (**Fig. 6a**) and BrdU incorporating cells (**Fig. 6b**) in a dose dependent manner. Then, it was investigated whether the ERK-1/2 activation is involved in the SP-stimulated cell proliferation or not (**Fig. 6c-e**). When SP was treated at the same time with fresh MSCGM change, ERK-1/2 activation was observed in both control culture and SP-treated culture at 15 min and 30 min but was sustained up to16 h post

treatment only in the SP treated culture, indicating that the serum-stimulated ERK-1/2 activation, overlapped at earlier time with SP-stimulated one, had completely returned to the basal level at 16 h but the SP-stimulated effect still remained (**Fig. 6c**). In order to investigate the ERK1/2 activation contributed only by SP treatment without overlapping ERK1/2 activation by the fresh medium change at early time point, SP was treated to human MSCs at 24 h after the fresh medium change, corresponding to the time when the serum-stimulated ERK-1/2 activation has been regressed to the basal level. Then, the time course of ERK-1/2 activation was re-examined (**Fig. 6d**). The SP-stimulated Erk-1/2 activation was initially detected at 30 min and regressed to basal level at 1 h and then much bigger ERK-1/2 activation reappeared at 16 h and again at 48 h, both of which were suppressed by MEK inhibitor PD98059 (**Fig. 6e**). This late and biphasic pattern of ERK-1/2 activation was probably not due to the SP-stimulated up-regulation of NK-1R in human MSC (**Fig. 6f**) or the persistent presence of SP in the culture medium (**Fig. 6g**).

In order to determine if SP affects the self-renewal capacity of human MSCs, β-catenin, a down stream effector of the wnt signaling pathway (39-41), was examined (**Fig. 6h**). At 16 h post treatment, β-catenin was mainly observed in the cytoplasm of human MSCs but small numbers of human MSCs only at 100 nM showed nuclear localization of β-catenin (data not shown). At 48 h post treatment, nuclear translocation of β-catenin was distinct particularly at 100 nM SP and almost all the human MSCs showed nuclear translocation of β-catenin (**Fig. 6h,** arrows). This SP-stimulated nuclear translocation of β-catenin was also confirmed when SP was treated under the serum-starved condition (**Supplementary Fig. 8** online). The induction of down stream genes of Tcf/β-catenin such as fibronectin (41) and VEGF was also shown by western blot analysis (**Fig. 6i**) and ELISA (**Fig. 6j**), respectively. This suggests that SP may play an additional role in the

repopulation of MSCs in the BM by stimulating self-renewal capacity via the well-known canonical wnt signaling pathway. (39). This event might be prerequisite for MSC mobilization, which took approximately 3 day after SP injection in the rabbit.

Discussion

Recent several reports regarding SP's diverse roles on the neuro-immune network in the BM (42), tumor cell proliferation *(*21, 22), BM fibrosis (29*)* and corneal-reepithelialization (32, 33) have been explored within the local environment of direct cellular contacts. Our finding in this study that SP may play roles as a messenger of the tissue injury as well as a MSC mobilizer from the BM opens up yet unidentified novel function of SP, acting systemically as a remote controller for the BM MSCs to be engaged in the tissue regeneration process. This function of SP was expected and supported from data; early detection of immunoreactive SP and its gene expression in the injured site, SP-detection in the PB and the wound size dependency of its induction kinetic, SP-dependent mobilization of $CD29^+$ MSC, and stimulation of wound healing by exogenous SP injection or MSC^{sp} cell transfusion after the alkali-burn on rabbit eye. In addition, the mechanism of SP-stimulated MSC mobilization from the BM was revealed in vitro by the transmigration of human MSC with concomitant induction of proteolytic enzymes and their BM origin also supported by detection of the injected AP-conjugated SP on the $CD29^+$ cell clusters of the BM flush. As expected from previously reported function of SP on the cell proliferation (22), SP stimulated ERK1/2 activation and nuclear translocation of β-catenin, which may then contribute to MSC repopulation in the BM to refill up the BM stroma. This is the first report that SP is a systemically acting wound messenger starting from the injured site, then to the circulation, and finally to the BM in order to mobilize the MSC from the BM stem cell reservoir into the circulation and to recruit to the injured area for tissue repair.

The SP, as a systemic messenger of the tissue injury, seems to be very specific to MSC mobilization. We demonstrated that the SP level in the PB is injury-inducible in the mouse (**Fig. 1a, b**) and also dependent on the wound size in the rabbit (**Fig. 2b**) and this injury-inducible SP or exogenous SP regulates MSC^{sp} mobilization kinetic (**Fig. 2c, d** and **Fig. 3c, e**). The specificity of SP on the MSC mobilization was shown by the data that exogenous SP treatment did stimulate HSC mobilization only 2 folds, comparing to 80 folds induction in MSC mobilization (**Fig. 2e,f**) and also did not stimulate macrophage mobilization (**Fig. 2d** and **Fig. 3d**). Furthermore, MSC mobilization in the PB seems to attenuate HSC-CFU

increase in the PB which is probably stimulated by the injury itself (**Fig. 3g**). All of those data strongly support that the SP is a specific MSC mobilizer.

The SP peptide at the early wound site may be initially provided by the corneal resident cells such as the trigeminal sensory neuron, epithelial cells, keratocytes, and endothelial cells but not by the infiltrating neutrophiles or macrophages since SP was detected at early stage of the inflammatory phase, disappeared in the injury site, and reappeared in the fibroplasia phase mainly among the migrating epithelial cells, endothelial cells and fibroblastic cells (**Supplementary Fig. 1** online). The wound size-dependency of SP kinetic in the PB (**Fig. 2b**) indirectly suggests that the SP in the wound site may be released into the circulation as a systemic injury messenger. However possible role of other late inflammatory cells or macrophages on SP secretion in the circulation as a secondary event initially starting from the SP in the wound microenvironment remains unresolved.

SP's role on neuro-immune communication was examined on hematopoietic modulation through its effect on stromal MSC (42), expected from innervation of SP nerve fibers in the BM stroma, expression of NK-1R in the BM MSC, and SP-dependent induction of SCF and IL-1 (28). However, circulatory SP's effect on the systemic mobilization of MSCs has not yet been reported previously.

Furthermore, SP-stimulated nuclear translocation of β-catenin and cell proliferation (**Fig. 6**) strongly suggest a more extended role of SP in the control of the MSC pool in the BM. These may also be important for the MSC repopulation after their mobilization as well as their ultimate feeder roles in the maintenance of hematopoietic microenvironment in the BM. Therefore, the systemic neuro-immune modulation from the injury inducible SP on hematopoiesis also has to be reconsidered in addition to its reported function on neuro-immunune modulation through the direct contact with SP nerve fibers (42).

The $CD29^+$ attached fibroblastic cells in the PB, which were mobilized by exogenous SP injection (**Fig. 1c** and **Fig. 2d, e**) or the injury inducible endogenous SP (**Fig. 2 c**), were MSCs probably derived from the BM. Our data of iv injected AP-conjugated SP's binding to the $CD29^+$ cell clusters of the BM flush 2 h post injection (**Fig. 1d,e**), suggests BM as a possible source of circulatory $CD29^+$ cells mobilized by SP injection. Distinct surface expression profiles of $CD\text{-}29^+$ cells in the

PB from those of macrophages, HSC, and EPC and their acquisition of fibroblastic morphology after the culture (**Fig. 2g,h** and **Supplementary Fig. 2** online) and multi-potent differentiation capacity (**Fig. 2i**) strongly support that those $CD29^+$ cells in the PB were MSC mobilized probably from the BM. However our data of constitutive K3 expression in the circulatory $CD29^+$ cells (**Fig. 2g.h**) and their preferential integration into the entire epithelial layer of the injured tissue after the transfusion (**Fig. 4c**) were not previously expected as known characteristics of MSC from the BM. This epithelial integration might occur through two events of the cell fusion and/or transdifferentiation as shown in the injured airway epithelium (43), the lung injury (7, 8), liver injury (12), and skin injury (9-11) but was not explored in detail in this study since molecular probes are quite limited in the rabbit. However, considering several previous reports on the epithelial transdifferentiation of MSC especially under the injury environment (43) and expression of other keratins in MSC under certain condition (9, 44) in addition to our data of K3 expression in human MSC as well as MSC^{sp}, MSC may have already retained the potential for epithelial transdifferentiation operating only transiently within the wound microenvironment.

Even though SP's importance on the wound healing has previously been suggested in the corneal wound healing (32, 33) and diabetic ulcer (31), it was mainly explored within the proximity of the injured site. Our data that MSC was mobilized into the PB by systemically injected SP or by injury-induced endogenous SP and the wound healing was accelerated by SP i.v. injection or the transfusion of MSC^{sp} also accelerated the wound healing, strongly supports that the mobilized $CD29^+$ cell, probably MSC from the BM, is an active participant for tissue regeneration. This new function of SP as a MSC mobilizer also has to be considered as a systemic injury messenger since this SP rise was initially recognized in the injured tissue just after the tissue damage.

In this study, factors responsible for trafficking of the $CD29^+$ cell to the injured tissue were not investigated but those factors such as HIF-1, SCF, PIGF, and VEGF noted by RT-PCR and ELISA (Figure 1 and data not shown) might be explored for possible candidates in the future study. However those well established mechanisms on SDF-1 dependent homing to the myocardially infracted tissue (15) after G-CSF stimulated EPC mobilization may not work in the $CD29^+$ cell homing to the injured tissue since most MSCs except a minor subset do not

express CXCR-4 (45).

Normative lag time for circulatory mobilization of MSC^{sp} in the rabbit might be approximately 3 days after the SP's peak in the circulation, similarly to the clinical protocol of the G-CSF stimulated $CD34^{+}$ progenitor mobilization, approximately 4-5 days. Under in vitro transmigration assay, SP-stimulated migration of human MSCs took approximately 3 days to accomplish the transmigration. Our biochemical data such as SP-stimulated cell proliferation, Erks activation, β-catenin nuclear translocation observed in human MSC, and AP-conjugated SP binding as early as 2 h post injection in the mouse strongly suggested that those sequential events ultimately lead to MSC mobilization from the BM during the lag period. In contrast, shorter lag time, approximately one day, was shown in the mouse, which may be reflected by the difference in species and body size.

SP is known to bind to the cell surface G-protein coupled receptor (GPCR), NK-1R and elicits a variety of responses such as inflammation and cell proliferation in T lymphocyte, skin fibroblasts, smooth muscle cells, and synoviocyte (46-48). Those pleiotrophic responses may be based on the GPCR mediated transactivation of the EGFR and subsequent ERK1/2 activation as previously reported in GPCR signaling pathway such as vassopressin and VIP (21-23). In this study, biphasic late ERK1/2 activation observed at 16 h and 48 h may not be due to the continuous and sustained activation of NK-1R since only 1/200 and 1/300 of the original SP dose in the case of 100nM SP were left 24 h and 48 h after the SP treatment respectively and NK-1R expression was fairly constant based on the western blot analysis during the SP treatment. This may be rather due to the secondary factors released by the primary SP response, which remains to be explored. The interrelationship between ERK1/2 activation, MMP induction, and cell migration, has to be determined but several previous reports strongly suggested that those sequential events might be plausible.

The high level of SP and NK-1R is associated with the metastatic and malignant phenotypes in several cancer cells (21, 22). Newly identified roles of SP in cell mobilization, MMP induction, cell proliferation, and possibly the β-catenin mediated self renewal capacity are also expected to interplay in the tumor

metastasis. Therefore, side effects such as neuro-inflammatory (49) effect and metastatic stimulation of SP, in addition to it's promising effects such as a wound healing agent and a cell therapeutic MSC mobilizer, needs to be considered and finely regulated for future clinical applications.

Materials and Methods

Materials

Primary human MSCs, mesenchymal growth medium (MSCGM; PT-3001), and chondrogenic differentiation medium (PT-3003), adipogenic induction medium (PT-3004), osteogenic induction medium (PT-3002) were purchased from Cambrex Bio Science. SP peptide, AP-conjugated SP, gelatin, and Millicell were purchased from Calbiochem, R&D system, Becton Dickinson, and Millipore respectively. Abs against CD34 (Cat # sc-9095), CD-29 (Cat # sc-6622, 1:200), c-kit (Cat # sc-1493, 1:100), CD45 (Cat # sc-1121, 1:50), CD 166 (Cat # sc-25624, 1:100), NK-1R (Cat # sc-15323, 1:100) and SP (Cat # sc-9758, 1:200) were purchased from Santa Cruz Biotechnology and Abs against α-SMA(DAKO, Cat # M0851, 1:50), CD105(DAKO, Cat # M3527, 1:50), CD44 (DAKO, Cat # M7082, 1:100), CD29 (DAKO, Cat # M0889, 1:100), and STRO-1 (R&D, MAB1038, 1:150), K3 (ICN, Cat # 69143, 1:200), β-catenin (BD, Cat # 610154, 1:100), ERK^{P} (Cell signaling Cat # 9102, 1:500), pan-ERK (BD Cat # 610123, 1:500) were purchased. The Abs against TIMP-1 (Cat # IM32L, 1:250), TIMP-2 (Cat # IM11L, 1:250), and MMP-9 (Cat # 444236, 1:100) were acquired from Calbiochem. The Abs against MMP-2 (Cat # MAB13405, 1:200) and MT1-MMP (Cat # MAB3319, 1:100) were purchased from Chemicon. ELISA kits for SP, VEGF, TNF-alpha, and IL-1beta were purchased from R&D system. Primary Abs were detected using ABC KIT, FITC or Texas Red-conjugated secondary antibodies (Vector), and HRP-conjugated secondary antibodies (Biorad). PKH red fluorescent cell linker kit (Cat # MINI26) was purchased from Sigma Chemicals. Type I-A collagen and type IV collagen were purchased from Nitta gelatin (JP). NK-1R blocker, RP67580 (Cat # 1635) and L732138 (Cat # 0868) were purchased from TOCRIS. HSC-CFU media (Cat # 130-091-280) was purchased from Miltenyi.

Alkali-burn eye animal model

Balb/c mouse weighing 25-30g were purchased from Jackson Lab (West Grove, PA) and New Zealand white rabbits weighing 2-3kg were purchased from Samtako BioKorea. All the animal experiments were approved by the ethical committees for

experimental animals of the Kyunghee University and the Chung-Ang University and conducted in accordance with the ARVO Statement for the Use of Animal in Ophthalmic and Vision Research. For the alkali burn, mouse eyes were placed in contact with the circular Whatman filter paper (3mm diameter) or Q-tips soaked in 1N NaOH for 10 seconds and excess NaOH rinsed out with the saline irrigation. For rabbits, the alkali burn was made with the circular filter paper (6 mm diameter) soaked in 1N NaOH for 10 seconds (**Fig. 2a**) and as previously described(18).

RT-PCR analysis

The RNA was isolated from the alkali burned mouse eye by Trizol (Cat # 15596-026, Invitrogen, Carlsbad, CA). A total of 1μg RNA was reverse transcribed (RT) using a reverse transcription-polymerase kit (Takara), which was followed by PCR using mouse gene-specific primers:

VEGF (expected size: 407), (sense) 5'GTACCTCCACCATGCCAAGT3', (antisense) 5'AATGCTTTCTCCGCTCTGAA 3',

TNF-alpha (expected size: 438), (sense) 5'GAACTGGCAGAAGAGGCACT3', (antisense) 5'GTGGGTGAGGAGCACGTAGT3',

IL-1 (expected size: 432), (sense) 5'GCTGCTTCCAAACCTTTGAC3', (antisense) 5'AGGCCACAGGTATTTTGTCG3',

SP (expected size: 309), (sense) 5'TCGATGCCAACGATGATCTA3', (antisense) 5'AGTTCTGCATTGCGCTTCTT3

HIF-1 alpha (expected size: 297), (sense) 5'GAAATGGCCCAGTGAGAAAA3', (antisense) 5'TATCGAGGCTGTGTCGACTG3'

VEGFR-1 (expected size: 414), (sense) 5'CTCAAGTGTCACCAGCTCCA3' (antisense) 5'GGGTATGGAGAACCCCCTAA3'

VEGFR-2 (expected size: 430), (sense) 5'CTGGGAGCTGGAAGACAAAG3' (antisense) 5'GTACCTCCACCATGCCAAGT3'

PlGF (expected size: 287), (sense) 5'TGCTGGTCATGAAGCTGTTC3' (antisense) 5'GCTGTCTTTATCGGCACACA3'

SCF (expected size: 329), (sense) 5'CCTCTCGTCAAAACCAAGGA3' (antisense) 5'GGCCTCTTCGGAGATTCTTT3'

β-actin (expected size: 415), (sense) 5'TGTTACCAACTGGGACGACA3' (antisense) 5'TTTGATGTCACGCACGATTT3'

For the rabbit MSC^{sp}, the RNA isolation and RT-PCR were followed as described above using rabbit gene-specific primers:
α-SMA (expected size: 455), (sense) 5'TTTCAATGTCCCAGCCATGT3' (antisense) 5'ATTCCATCCCGATGAAGGAG
CD29 (expected size: 473), (sense) 5'TGTATACAAGCAGGCCCCAA3' (antisense) 5' TTCTCTGCTGTGCCTTTGCT3'
K3 (expected size: 314), (sense) 5' CTCAATGTGGAGATCGACCC3' (antisense) 5' AGGTCCTGCATGCTTCTCAG3'
GAPDH (expected size: 459), (sense) 5' GAAGGTCGGAGTGAACGGAT3' (antisense) 5' TGCGTTGCTGACAATCTTGA3'

SP-dependent $CD29^+$ cell mobilization

SP (5nmole/kg) was i.v. injected into the mouse tail vein or rabbit ear vein and the blood was collected at the indicated time. After removing red blood cells by Ficoll gradient centrifugation, mononuclear cell fraction was allowed to attach for 1 day and unbound lymphocytes were removed at the first medium change. The attached cells were either fixed for immunocytochemical staining or further cultured in MSCGM until obvious fibroblastic morphology and cell growth resume. The cells were stained with mouse specific Abs against CD29, CD166, CD117, α-SMA, CD34 and CD45 or rabbit specific Abs against CD29, α-SMA, CD45, and K3 and subsequently detected by FITC or Texas Red conjugated secondary Abs. For the specificity confirmation of CD29 and CD45 as surface markers to distinguish MSC from macrophage among attached PB cells, mouse peritoneal macrophage was used.

AP-conjugated SP binding to the BM cells

AP-conjugated SP was i.v. injected to mouse tail vein and at 0 h, 2 h, and 4 h post injection, mouse femur was irrigated with collagenase solution and the isolated cells were allowed to attach in MSCGM for 24h. AP activity was measured according to the manufacturer's specifications (Sigma Chemical) and after examination of AP activity, the cells were fixed for immunocytochemical staining with CD29 Ab. In order to rule out endogenous AP activity and also SP-stimulated induction of AP activity in the BM-MSC, human MSCs purchased from Cambrex were treated with SP and their AP activity was measured as described above.

The wound-size dependency of the SP induction and MSC mobilization

One wound per eye (total two wounds per rabbit) or two wounds per eye (total four wounds per rabbit) were made as shown in Figure 2a. For two wounds per eye, both wounds were made on the upper part of the eye with approximately 90 degree separation not to overlap with the muscular tendon of the middle line. For ELISA of SP in the serum, 1.5ml of PB was collected at 1h, 6h, 24h, 48h and 72h post burn from the same rabbit. To monitor the numbers of MSC in the PB, 10ml PB was collected sequentially at 3, 5 and 7 days post burn from the same rabbit and the $CD29^+$ attached cells were counted after the two week culture.

Effect of SP i.v. injection on MSC and HSC mobilization and on the wound healing

One wound per eye (3 per group) was made as described above and SP at doses of 0.05 nmole/kg, 0.5 nmole/kg, 5.0 nmole/kg were i.v. injected twice just after the injury and 1 day. PB 10ml was collected at 0, 3, 5, 7, 9 days from the same rabbit and mononuclear cells were isolated by Ficoll gradient centrifugation. For MSC counting, the cells were allowed to be attached and after removal of lymphocytes were cultured in MSCGM for 2 weeks and fixed in 4% paraformaldehyde. Double immunofluorescence staining for CD45 and CD29 and for α-SMA and CD29 along with DAPI staining was performed. CD29+ cells were counted For HSC-CFU assay, the cells were cultured HSC-CFU media for 2 weeks and colonies were counted. For molecular characterization of the mobilized cells, RT-PCR and immunofluorescence staining was performed as described above. Effect of SP injection on the wound healing was monitored by Digital camera and by H&E staining of the fixed tissue.

Multipotent differentiation capacity of the mobilized $CD29^+$ cells

For multi-potent differentiation capacity test of mobilized cells, the cells from SP injected 3 day post burn were subcultured in MSCGM for 4 weeks. All the macrophages were removed at the first passage by trypsin sensitivity. For adipogenic differentiation capacity, $2x10^5$ cells/well were cultured in DMEM-high glucose (Gibco) supplemented with 0.5 mM 1-methyl-3-isobutylxanthine (Sigma),

1 μM dexamethasone (Sigma), 10 μg/ml insulin (Sigma), and 10% FBS for 21 days and the fixed cells were stained with oil red "O". For osteogenic differentiation capacity, $4x10^4$ cells/well were cultured in DMEM-high glucose (Gibco) supplemented with 1 μM dexamethasone (Sigma), 0.05 mM ascorbic acid (Sigma), 10 mM β-glycerophosphate (Sigma), and 10% FBS for 21 days and stained with Alizarin red. For chondrogenic differentiation capacity, 5 $x10^5$ cells/well were incubated in chondrogenic differentiation medium (Cambrex) in 15ml polystyrene tube for 4 week and the chondrocyte pellets were fixed with 4% paraformaldehyde for 48h. The sections were stained in Weigert's iron hematoxylin and Safranin-O. As a positive control, the same induction was applied to human MSC.

Autologous MSC^{sp} transfusion

The SP-stimulated mobilized cells were isolated from the 3 day PB of unburned rabbits and were individually cultured for 4 weeks. For PKH-labeling, cells were prepared in a conical bottom polypropylene tube and washed once using serum-free medium and labeled using PKH red fluorescent cell linker kit (Sigma) according to manufacturer's specifications. At 3 day after the burn injury, approximately corresponding the start time of MSC mobilization after the SP injection, PKH labeled cells ($5x10^6$ cells) were transfused through the rabbit ear vein. At 7 day, all the rabbit were sacrificed and the eyes were embedded in OCT.

Frozen sections (5 μm) were incubated with either K3, CD29, and α-SMA Ab after blocking with normal goat serum and then with FITC-conjugated secondary antibodies. After DAPI staining, sections were mounted with vector shield and PKH labeled cells and FITC labeled cells were observed immediately with fluorescence stereomicroscope (Leica) or confocal microscope (Zeiss)

Cell culture

Human MSCs (Cambrex) were cultured in the MSCGM and the medium was changed every three days. The MSCs between passage 4 and 6 were used for all the in vitro experiments and their identity was confirmed at each passage by the expression of CD105, CD44, CD29, and STRO-1.

In vitro cell migration assay

The type I collagen gel matrix was made within a 12 mm millicell membrane (12-μm pore size) according to the manufacturer's specifications (Nitta gelatin, Japan) and coated overnight with type IV collagen (Nitta gelatin). The MSCs were plated on top of the collagen gel. SP and human specific NK-1R blocker, L732138 (100 nM) were treated either in the upper or the bottom chamber. The clearance of the collagen gel was examined. The millicell inserts were fixed 3 day, and stained with H&E. The culture supernatants were saved for the gelatin zymography.

Gelatin zymography

The culture supernatant was resolved in the 8 % SDS-PAGE under non reducing condition, the gel was renatured with 2.5% Triton x-100 to order to remove the SDS, incubated with a developing buffer (50 mM Tris-HCl, pH 7.2 100 mM NaCl, 20 mM $CaCl_2$) at 37°C overnight, and the gel was stained with Coomassie blue.

Metabolic cell labeling and immunoprecipitation

Human MSCs were treated with SP and labeled with 50 μCi/ml ^{35}S-methionine (Amersham) for 16 h. The cell lysate was prepared with a lysis buffer (1% NP40, 10 mM Tris-HCl, pH 7.4, 150 mM NaCl. 1 mM EDTA, 2 mM PMSF). For immunoprecipitation of the secreted MMP-1, MMP-2, MMP-9, TIMP-1, and TIMP-2, the culture supernatants were incubated with their specific antibodies for 2 h under constant rotation and the antibodies were collected by protein-G sepharose-4B (Biorad). The pellet was washed three times with an immunoprecipitation buffer (150 mM NaOH, 50 mM Tris-HCl pH 7.4, 0.2% SDS and 0.5% Nadeoxycholate), once with a high salt buffer (10 mM Tris-HCl, pH 7.4, 0.5 M NaCl), and once with a low salt buffer (10 mM Tris-HCl, pH 7.4). After SDS-PAGE, the gel was soaked in 2 M sodium salicylate, dried, and exposed to the X-ray film for 2 weeks. For immunoprecipitation of MT1-MMP, membrane bound MMP-2, TIMP-2, and TIMP-1, the cell lysate was incubated with specific primary antibodies and the remaining procedures were the same as described above.

Western blot analysis

Human MSCs were lysed with the lysis buffer containing 50 mM sodium vanadate. After SDS-PAGE, the proteins were transferred to a nitrocellulose membrane at 250 mV for 2h. The membrane was blocked with 5% skim milk (Becton Dickinson),

incubated with the antibodies against MT1-MMP, phospho-ERK, pan-ERK, NK-1 R, and α-tubulin for 90min, and developed by a the chemiluminescence detection kit (NEN)

BrdU labeling

Human MSCs were cultured with SP on cover slip for 24h and 48h. BrdU was added to humans MSCs at 2h before the cell harvest. Humans MSCs was fixed with absolute methanol for 10min and DNA was denatured by incubation with HCl (2M) for 60min. For neutralization, cover slips were immersed with Borate buffer (0.1M, pH 8.5) twice over a 10min period and washed with PBS three times. Cover slips were incubated with anti-BrdU antibody for 60min at RT and then with the FITC-conjugated secondary antibodies. The cells were counterstained with DAPI and examined with confocal microscope (Leica)

Acknowledgements

This research was supported by a grant (SC3120) from Stem Cell Research Center of the 21st Century Frontier Research Program funded from the Ministry of Science and Technology (MOST) and in part by Musculoskeletal Bioorgan Center funded from Ministry of Health and Welfare and by Korea Atomic R&D Fund from MOST, Republic of Korea, given to Professor Youngsook Son.

Reference

1. Lim M, Goldstein MH, Tuli S, Schultz GS. Growth factor, cytokine and protease interactions during corneal wound healing*. The ocular surface*. **1,** 53-65 (2003).
2. Xinan L, Suguang L, Liangchao Z, Lei C.. Change in Substance-P in a firearm wound and its significance. *Peptides* **19,** 1209-1212 (1998).
3. Orlic D, Kajstura J, Chimenti S, Bodine DM, Leri A, Anversa P. Bone marrow cells regenerate infarcted myocardium. *Nature* **410,** 701-705 (2001).
4. Hiroshi Kawada *et al.* Nonhematopoietic mesenchymal stem cells can be mobilized and differentiated into cardiomyocytes after myocardial infarction. *Blood* **104,** 3581-3587 (2004).
5. Young-sup Yoon *et al.* Clonally expanded novel multipotent stem cells from human bone marrow regenerate myocardium after myocardial infarction. *J. Clin. Invest*. **115,** 326-338 (2005).
6. Toma C, Pittenger MF, Cahill KS, Byrne BJ, Kessler PD. Human mesenchymal stem cells differentiate to a cardiomyocyte phenotype in adult murine heart. *Circulation* **105,** 93-98 (2002).
7. Mauricio Rojas *et al.* Bone marrow-derived mesenchymal stem cells in repair of the injured lung. *Am J Respir Cell Mol Biol*. **33,**145-52 (2005).
8. Ortiz LA *et al.* Mesenchymal stem cell engraftment in lung is enhanced in response to bleomycin exposure and ameliorates its fibrotic effect. *Proc Natl Acad Sci USA*. **100,** 8407-8411 (2003).
9. Yaojiong Wu, Liwen Chen, Paul G Scott, Edward E Tredget. Mesenchymal stem cells enhance wound healing through differentiation and angiogenesis. *Stem cells*. Epublication (2007).
10. Susan R. Opalenik, Jeffrey M. Davidson. Fibroblast differentiation of bone marrow-derived cells during wound repair. *FASEB. J.* **11,** 1561-1563 (2005).
11. Li H *et al*. Adult bone–marrow–derived mesenchymal stem cells contribute to wound healing of skin appendages. *Cell Tissue Res.* **326,** 725-736 (2006).
12. Yasushi Sato *et al.* Human mesenchymal stem cells xenografted directly to rat liver are differentiated into human hepatocytes without fusion. *Blood* **106,** 756 – 763 (2005)
13. Powell TM *et al.* Granulocyte colony-stimulating factor mobilizes functional

endothelial progenitor cells in patients with coronary artery disease. *Arterioscler Thromb Vasc Biol*. **25,** 296-301 (2004).

14. Deng Z *et al*. Effects of GM-CSF on the stem cells mobilization and plasma C-reactive protein levels in patients with acute myocardial infarction. *Int J Cardiol*. **113,** 92-6 (2006).
15. Askari A. T. *et al.* Effect of stromal-cell-derived factor-1 on stem cell homing and tissue regeneration in ischemic cardiomyopathy. *Lancet*. **362,** 697-703 (2003*).*
16. Ceradini DJ. *et al.* Progenitor cell trafficking is regulated by hypoxia gradient through HIF-1 induction of SDF-1*. Nature med*. **10,** 858-864 (2004).
17. Rodriguez AM, Elabd C, Amri EZ, Ailhaud G, Dani C. Human adipose tissue is a source of multipotent stem cells*. Biochimie*. **13,** 4279-4295 (2002).
18. J Ye, K Yao, JC Kim. Mesenchymal stem cell transplantation in a rabbit corneal alkali burn model: engraftment and involvement in wound healing. *Eye* 1-9 (2005).
19. Susan R. Opalenik, Jeffrey M. Davidson. Fibroblast differentiation of bone marrow-derived cells during wound repair. *FASEB. J.* **11,** 1561-1563 (2005).
20. Ye J, Song YS, Kang SH, Yao K, Kim JC. Involvement of bone marrow-derived stem and progenitor cells in the pathogenesis of pterygium. *Eye* 1-5 (2004).
21. Alia Al-Sarraj and Gerand Thiel. Substance P induced biosynthesis of the zinc finger transcription Egr-1 in human glioma cells requires activation of the epidermal growth factor receptor and of extracellular signal-regulated protein kinase*. Neurosci.* **332,** 111-114 (2002).
22. Ignazio Castagliuolo, Leyla Valenick, Jeniffer Liu, Charalabos Pothoulakis. Epidermal growth factor receptor transactivation mediates substance P-induced mitogenic responses in U-373 MG cells. *J Bio Chem.* **275,** 26545-26550 (2000).
23. Yang CM *et al*. Substance P – induced activation of p42/44 mitogen-activated protein kinase associated with cell proliferation in human tracheal smooth muscle cells. *Cellular signaling* **14,** 913-923 (2002).
24. Rameshwar P., Ganea D., Gascon P. In vitro stimulatory effect of Substance-p on hematopoiesis. *Blood* **81,** 391-398. (1993).
25. Michifumi Watanabe, Kiyo Nakayasu, Minoru Iwatsu, Atsushi Kanai.

Endogenous substance P in corneal epithelial cells and keratocytes. *JPN. J. Opthalmol*. **46,** 616-620 (2002).

26. Ho W. Z., Lai J. P., Zhu X. H., Uvaydova M., Douglas S. D. Human monocytes and macrophages express substance P and neurokinin-1 receptor. *J. Immunol.* **159,** 5654–5660 (1997).
27. Singh D *et al*. Increased expression of preprotachykinin-I and neurokinin receptors in human breast cancer cells: Implications for bone marrow metastasis. *PNAS.* **97,** 388-393 (2000).
28. Pranela Rameshwar and Pedro Gascón. Substance P (SP) Mediated Production of stem cell factor and interleukin-1 in bone marrow: potential autoregulatory role for these cytokines in SP receptor expression and induction. *Blood* **85,** 482-490 (1995).
29. Rameshwar P *et al*. Mimicry between neurokinin-1 and fibronectin may explain the transport and stability of increased substance P immunoreactivity in patients with bone marrow fibrosis. *Blood* **97,** 3025-3031 (2001).
30. Olerud JE *et al*. Neutral endopeptidase expression and distribution in human skin and wounds*. J Invest Dermatol*. **112,** 873-881 (1999).
31. Antezana M *et al*. Neutral endopeptidase activity is increased in the skin of subjects with diabetic ulcers. *J Invest Dermatol*. **119,** 1400-1404 (2002).
32. Nakamura M. *et al.* Promotion of corneal epithelial wound healing in diabetic rats by the combination of a substance P-derived peptide (FGLM-NH2) and insulin-like growth factor-1. *Diabetologia* **46,** 839-842 (2003).
33. Yamada N, Yanai R, Nakamura M, Inui M, Nishida T. Role of the c domain of IGFs in synergistic promotion, with a substance P-derived peptide, of rabbit corneal epithelial wound healing. *Invest. Opthalmol. Vis. Sci.* **45,** 1125-1131 (2004).
34. Tschachler E. *et al.* Sheet preparations expose the dermal nerve plexus of human skin and render the dermal nerve end organ accessible to extensive analysis. *J Invest Dermatol*. **122,** 177-182 (2004).
35. Miller A., Costa M., Furness J. B., Chubb I. W. Substance p immunoreactive sensory nerves supply the rat iris and cornea. *Neurosci. Lett*. **23,** 243-249 (1981).
36. Gallar J., Pozo MA, Rebollo I, Belmonte C. Effects of capsaicin on corneal

wound healing. *Invest Ophthalmol Vis Sci*. **31,** 1968-74 (1990).
37. Park KS *et al*. The side population cells in the rabbit limbus sensitively increased in response to the central cornea wounding. *Invest Ophthalmol Vis Sci*. **47,** 892-900 (2006).
38. Toth M, Chvyrkova I, Bernardo MM, Hernandez-Barrantes S, Fridman R. Pro-MMP-9 activation by the MT1-MMP axis and MMP-3: role of TIMP-2 and plasma membranes. *Biochem. Biophys. Res. Commun.* **308,** 386-395 (2003).
39. De Boer J, Wang HJ, Van Blitterswijk C. Effects of Wnt signaling on proliferation and differentiation of human mesenchymal stem cells. *Tissue eng.* **10,** 393-401 (2004).
40. Reya T *et al*. A role for Wnt signalling in self-renewal of hematopoietic stem cells. *Nature* **423,** 409-414 (2003).
41. Gradl, D., Kuhl M., Wedlich D. The Wnt/Wg signal transducer beta-catenin controls fibronectin expression. *Mol Cell Biol.* **19,** 5576-5587 (1999).
42. Rameshwar P *et al*. The dynamics of bone marrow stromal cells in the proliferation of multipotent hematopoietic progenitors by substance P: an understanding of the effects of neurotransmitter on the differentiating hematopoietic stem cell. *J. Neuroimmunol.* **121,** 22-31 (2001).
43. Spees JL. *et al.* Differentiation, cell fusion, and nuclear fusion during *ex vivo* repair of epithelium by human adult stem cells from bone marrow stroma. *PNAS.* **100,** 2397-2402 (2003).
44. Wu M. *et al*. Differentiation potentials of human embryonic mesenchymal stem cells for skin-related tissue. *Br J Dermetol*. **155,** 282-291 (2006).
45. Wynn RF *et al*. A small proportion of mesenchymal stem cells strongly expresses functionally active CXCR4 receptor capable of promoting migration to bone marrow. *Blood* **104,** 2643-2645 (2004).
46. Payan, DG., Brewster DR., Goetzl EJ. 1983. Specific stimulation of human T lymphocytes by substance P. *J Immunol*. **131,** 1613-1615.
47. Nilsson J., Von Euler AM., Dalsgaard CJ. Stimulation of connective tissue cell growth by substance P and substance K. *Nature* **315,** 61-63 (1985).
48. Lotz, M., Carson DA., Vaughan JH. Substance P activation of rheumatoid synoviocytes: neural pathway in pathogenesis of arthritis. *Science* **235,** 893-895 (1987).

49. Kidd BL, *et al*. Inhibition of inflammation and hyperalgesia in NK-1 receptor knock-out mice. *Neuroreport* **14,** 2189-2192 (2003).

Figure legends

Figure 1 SP-expression in the alkali-burned mouse eye, subsequent SP-detection in the PB, and SP-stimulated mobilization of $CD29^+$ cells from the BM. (**a**) RT-PCR analysis of the injured mouse eye and (**b**) ELISA of the PB at the indicated time after the alkali burn on mouse eye. Results shown are mean values ± s. d. (n=4 at indicated time point). (**c**) SP-stimulated mobilization of $CD29^+$ cells and its inhibition by NK-1R blocker RP67580 in uninjured mice. SP at dose of 5.0nmole/kg was i.v. injected and the whole blood was withdrawn with heparin-coated syringe. After removal of unattached lymphocytes, round shaped and large attached $CD29^+$ cells were counted (**Supplementary Figure 2** online). For the analysis of SP specificity, NK-1R blocker RP67580 (0.5 μmole/kg) was co-injected with SP. Results shown are mean values ± s. d. (n=5 at the indicated time point). $*P < 0.05$ $**P < 0.01$, $***P < 0.001$ versus the PBS-injected control. I indicated coinjection of NK-1R blocker RP67580. (**d, e**) SP-binding on the attached $CD29^+$ cell clusters of the BM flush. AP-conjugated SP was i.v. injected and the BM flush from the tibia were collected at 0h, 2h, and 4h. After attachment of the BM flush, AP activity was measured in live cells. For detection of AP activity within the $CD29^+$ cell clusters of the BM flush, the same cover slip was fixed after AP color development and stained with CD29 Ab. Scale bar=100μm.

Figure 2 Wound-size dependency of SP induction in the PB and $CD29^+$ cell mobilization in the alkali-burned rabbit, SP-specific mobilization of $CD29^+$ cells in uninjured rabbit, and their reveal of multipotent MSC phenotype. (**a**) Alkali-burn rabbit eye model. One wound per eye (total two wounds per rabbit) or two wounds per eye (total four wounds per rabbit) were made by contacting the 1.0 N NaOH soaked circular paper. The injured site was noted as a white circle with hemorrhagic area. (**b**) Comparison of SP induction kinetics between two wound group (n= 5) and four wound group (n=5). Unburned rabbit as negative control (n=3). Results shown are mean values ± s. d. (**c**) Comparison of $CD29^+$ cell mobilization kinetics between two wound group (n=5) and four wound group (n=5). 10 ml PB was withdrawn sequentially from the same rabbit at the indicated time and $CD29^+$ fibroblastic cells were counted after the acquisition of fibroblastic

morphology for 15 day culture. In two wound per eye, all five rabbits showed $CD29^+$ cell mobilization in the PB at 5 day after the injury but no rabbit in one wound per eye showed $CD29^+$ cell mobilization at this time point. RB; rabbit (**d**) SP-stimulated mobilization of $CD29^+$, $CD45^-$ fibroblastic cells in uninjured rabbit without stimulation of $CD29^-$, $CD45^+$ macrophage. SP at dose of 5.0nmole/kg was i.v. injected twice and 10 ml PB was collected on 3 day and 7 day. After acquisition of fibroblastic morphology, double immunofluorescence staining with anti-CD45 (Texas Red; red) and anti-CD29 (FITC; green) was done. At 3 day after SP injection, $CD29^+$ cells were detected in the PB of uninjured rabbits. All the $CD29^+$ cells were negative in CD45 and $CD45^+$ macrophage in the PB did not increase. (**e**) Quantitative comparison of SP-stimulated mobilization of $CD29^+$, $CD45^-$ fibroblastic cells and (**f**) HSC-CFU. The PB was withdrawn 3 day after SP injection. $CD29^+$ attached cells after 14 day culture and HCS-CFU was counted. Results shown are mean values $\pm$ s. d. (n=5 in each group). (**g**) Molecular characterization of $CD29^+$, $CD45^-$ cells mobilized by SP injection in the uninjured rabbit by immunofluorescence staining, (**h**) by RT-PCR, and (**i**) by multipotent differentiation capacity. The $CD29^+$ cells mobilized into PB at 3 day after SP injection were cultured 4weeks. Macrophages were removed at first passage by their less sensitivity to trypsin. All the $CD29^+$ cells were α-SMA^+, $CD45^-$, $K3^+$ cells, which could be differentiated into adipocyte, osteoblast, and chondrocyte (n=4 in each group). Human MSC was used as a positive control. Scale bar=100μm.

Figure 3 Accelerated wound healing by SP injection was accompanied by accelerated MSC^{sp} mobilization and earlier regression of HSC-CFU in the PB. One wound per eye was made and SP or PBS was injected twice just after the burn and 1 day post burn at the dose of 5 nmole /kg. (**a**) Gross view of wound healing and (**b**) histological comparison between SP injected and PBS injected group (n=3 in each group). The original wound size was noted by the dotted circle. In the SP injected rabbit, transparent corneal surface with no hemorrhagic zone was observed, comparing to persistence of hemorrhagic zone in the PBS-injected rabbit. Macrophages and polymorphonuclear giant cells just beneath the limbus epithelium of the SP-injected group were noted (*) and actively infiltrating $CD29^+$ fibroblasts (arrows) were noted in the PBS-injected burn control. **(c)** Comparison of initial time of $CD29^+$, α-SMA^+ cell mobilization between the SP-injected and the

PBS-injected group by double immunofluorescence staining with anti-α-SMA (FITC; green) and anti-CD29 (Texas Red; red). 10 ml PB was sequentially withdrawn at indicated time after the injury and attached mononuclear cells were fixed after the acquisition of fibroblastic morphology. Total cells were visualized by DAPI staining. $CD29^+$, α-SMA^+ cells were detected at 3 day post burn in the SP-injected group but detected at 7 day in the PBS-injected burn control. (**d**) Comparison of mobilization kinetics of $CD29^+$, $CD45^-$ cells with those of $CD29^-$, $CD45^+$ macrophage between the SP-injected and the PBS-injected group by double immunofluorescence staining with anti-CD45 (Texas Red; red) and anti-CD29 (FITC; green). Mobilization of $CD29^-$, $CD45^+$ macrophages was not affected by SP injection in contrast to marked acceleration of $CD29^+$, $CD45^-$ cell mobilization by SP injection. (**e**) SP-dose dependency of MSC^{sp} mobilization kinetics. One wound per eye was made and SP was injected twice at the doses of 0.05nmole/kg, 0.5nmole/kg, and 5.0nmole/kg SP and 10 ml PB was withdrawn from the same rabbit sequentially four times at 3, 5, 7, 9 days post burn. $CD29^+$ cells in 10 ml PB were counted. Results shown are mean values $\pm$ s. d. (n=3 in each group). (**f**) Characterization of mobilized $CD29^+$ cells with RT-PCR. Molecular nature of the mobilized cells ($CD29^+$, α-SMA^+, $K3^+$) was identical even though their mobilization kinetics was distinct. (**g**) Effect of SP dose on HSC-CFU kinetics. From the PB withdrawn at indicated time, HSC-CFU was measured. Results shown are mean values $\pm$ s. d. (n=3 in each group). $^*P < 0.05$ $^{**}P < 0.01$, $^{***}P < 0.001$ versus the burn control.

Figure 4 Accelerated wound healing by autologous MSC^{sp} transfusion and their engraftment in the epithelial layer and stroma of the injured tissue. MSC^{sp} was isolated from 10 ml PB of six uninjured rabbits at 3 day after SP injection (5.0nmole/kg) and cultured individually in the MSCGM medium for 4 weeks. After immunofluorescence staining and RT-PCR analysis for the confirmation of cellular identity ($CD29^+$, α-SMA^+, $K3^+$, $CD45^-$), cells were harvested and labeled with PKH and $5X10^6$ $MSCs^{sp}$ were transfused through the ear vein of four rabbits, individually, at 3 day after the alkali burn injury (one wound per eye). The wound healing rate in the transfused group was compared with that of the PBS-injected burn control as well as the SP-injected group (n=4 per group). (**a**) Gross and histological view of

the wound healing effect of the MSC^{sp} cell transfusion in comparison with the SP injection and the PBS-injected burn control at 7 day post injury. Representative digital images from four individuals were shown. The original wound area was marked by the dotted circle. Histology of the entire area of the injured site was shown. cc, central cornea; Lim, limbus. At high magnification (**b**), rather loosely aggregating cells, indicative of upward migration of cells from the stroma (arrows), were detected in several locations at the borderline between the epithelial and stromal layer. (**c**) Immunofluorescence staining with K3, CD29 and α-SMA Abs in the $MSCs^{sp}$ transfused group, (**d**) in uninjured collateral side, (**e**) in PBS-injected burn control, and (**f**) in the SP-injected group as a positive control. Frozen sections were incubated with primary Abs and then FITC-labeled secondary Abs for concomitant detection of PKH-labeled cells in the same tissue sections. Total cells were visualized by DAPI staining. The PKH labeled MSC^{sp} was observed in the entire corneal epithelial layer and partly in the stroma. No PKH-labeled cell was noted in the uninjured collateral side. PKH negative $K3^{+}$ cells (*) were detected in the stroma of the injured region of cell transfused group, suggesting infiltration of endogenous MSC mobilized by the injury-induced SP. Scale bar=100μm

Figure 5 Transmigration of human MSCs on 3-D collagen gel accompanied by concomitant induction of MMPs and inhibition of TIMPs. (**a**) Transmigration of human MSCs on the 3-D collagen gel within a millicell insert. Human MSC were cultured on the type IV collagen-coated type I collagen gel matrix and were stimulated to migrate out of the gel along the SP-gradients by daily treatment of SP for 3 days. The transmigration and collagen degradation was noted by the clearance of the opaque collagen gel and also by the histological examination of the cross sections. Human MSCs in the gel were noted by arrows. (**b**) Gelatin-zymography of the culture supernatant. MMP-9 (92 kDa), MMP-2 (72 kDa), their activation-cleaved products were shown as clear zones in the gelatin-impregnated gel. (**c**) Blockade of chemoattractive transmigration of human MSC by abolishment of SP-gradient or NK-1 receptor blocker. To confirm chemokine-stimulated transmigration, the same concentration of SP (100 nM) was applied to the top and/or the bottom of the millicell chamber or the NK-1R blocker, L732138 (100nM) concomitantly with SP treatment for 3 days. (**d**) Effect of SP on the biosynthesis of

MMPs and TIMPs. Human MSCs were treated with SP and labeled with ^{35}S-methionine for 16h and the culture supernatants were subjected to immunoprecipitation with specific antibodies. (**e**) Effect of SP on the MT-1 MMP expression and membrane association of MMP-2 and TIMP-2. Triton X-100 soluble cell lysates were subjected to immunoprecipitation with specific Ab or western blot analysis. (**f**) Immunofluorescence staining with MT1-MMP. Human MSCs were treated with SP for 16 h, fixed, and stained with the MT1-MMP Ab and detected with FITC-conjugated secondary antibodies. MT1-MMP surface staining was increased by the SP treatment.

Figure 6 SP-stimulated cell proliferation, biphasic ERK1/2 activation, and nuclear translocation of β-catenin in human MSC. (**a**) The tryphan blue excluded viable cells were counted 3 day after the SP treatment. Results shown are mean values ± s. d. of four independent experiments. (**b**) BrdU labeling index after 24 h and 48 h SP treatment. The cells were incubated with BrdU for first 24 h or next 24 h after SP treatment. Results shown are mean values ± s. d. of two independent experiments. (**c**) Western blot analysis with anti-phospho-ERK-1/2 and anti-pan ERK Ab in the cell lysates of the SP-treated human MSCs, (**d**) in order to distinguish the SP-stimulated ERK-1/2 activation from the serum-stimulated one, SP was treated at 24 h after the fresh medium change when the serum-stimulated ERK-1/2 activation has regressed to the basal level. Early ERK1/2 activation at 30 min was followed by bigger biphasic ERK-1/2 activation at 16 h and 48 h post treatment. (**e**) PD98059 MEK inhibitor (50μM) inhibited upstream molecule for SP-stimulated ERK-1/2 activation. (**f**) Western blot analysis with anti-NK-1R Ab in the Triton X100 soluble cell lysates. (**g**) SP-ELISA in the culture medium after 24 h and 48 h treatment. SP at 100 nM remained 1/200 of original concentration and SP at 10 nM remained 1/40 after 24 h in the MSC culture. Results shown are mean values ± s. d. of four independent experiments. (**h**) Immunofluorescence staining with β-catenin Ab and FITC-conjugated secondary Ab. Human MSC was treated with SP and fixed at 48 h after SP treatment. Nuclear translocation of β-catenin was distinct at 48 h in all the cells of the SP 100 nM treated group. (**i**) ELISA for VEGF in the culture supernatant of SP-treated human MSCs for 48 h. Results shown are mean values ± s. d. of two independent experiments. (**j**) Western blot analysis for fibronectin in the culture supernatant of human MSCs cultured in the

presence of SP for 48 h. *P< 0.05 **P < 0.01, ***P < 0.001 versus PBS-treated control.

Figure 1

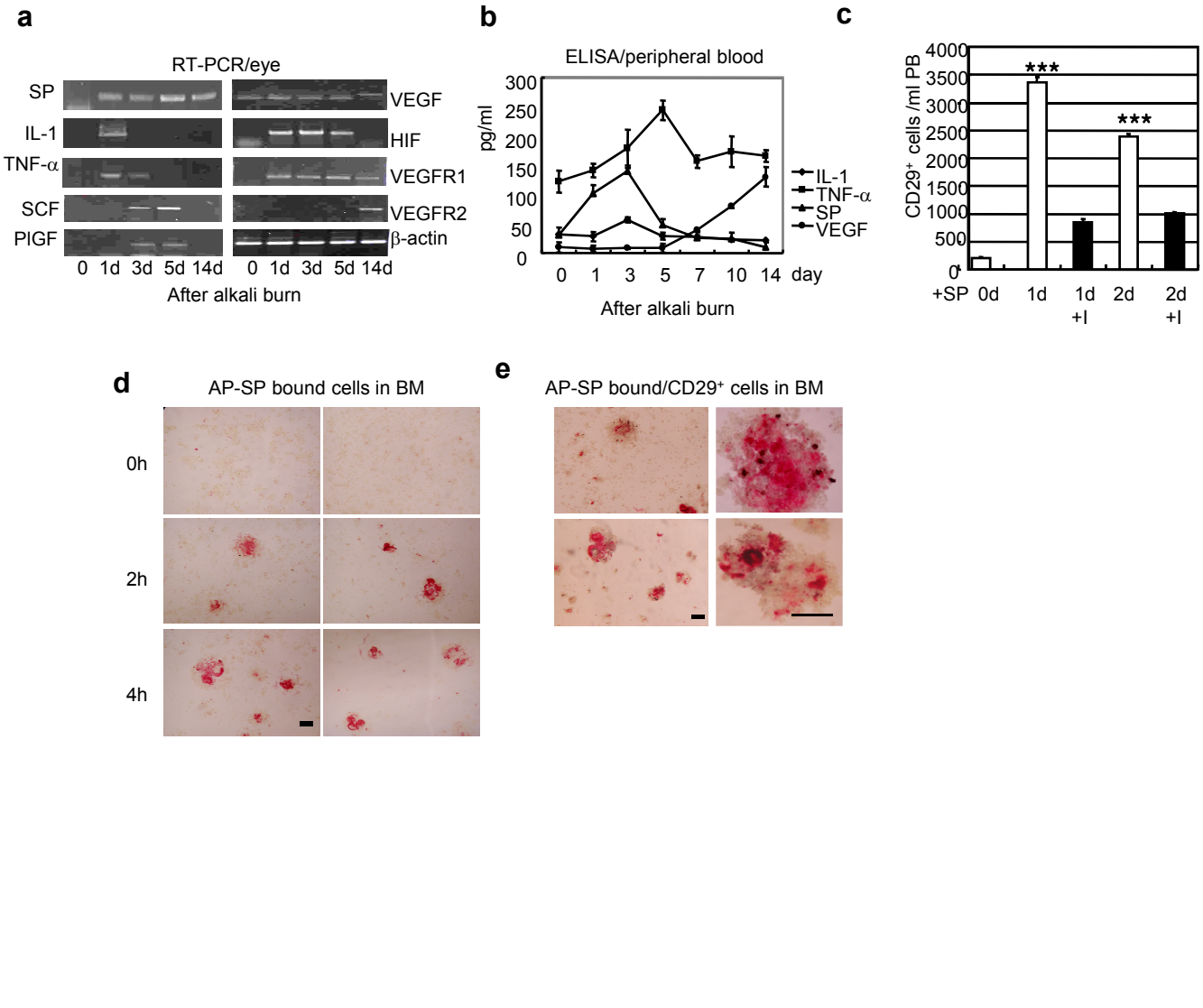

Figure 2

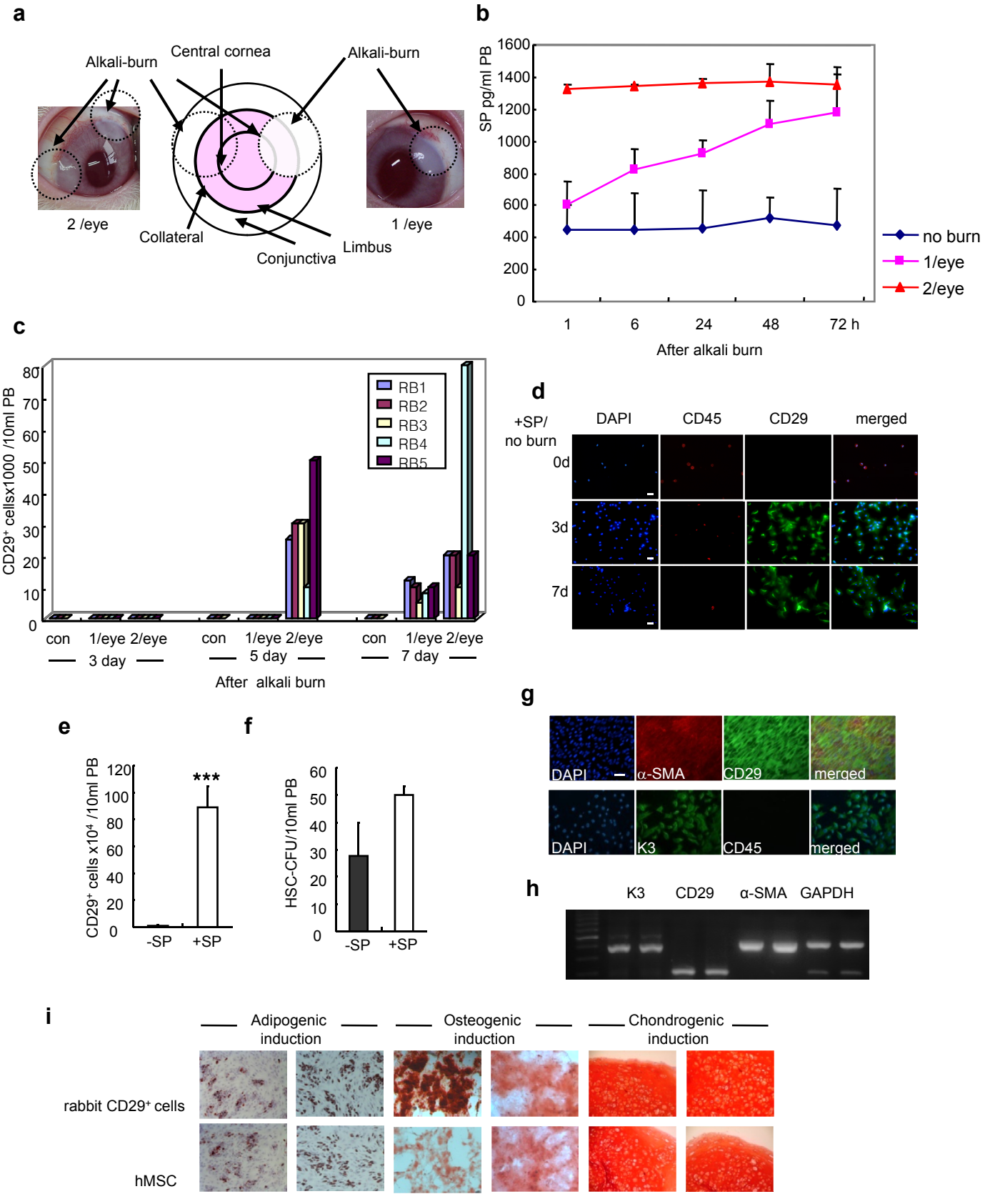

Figure 3

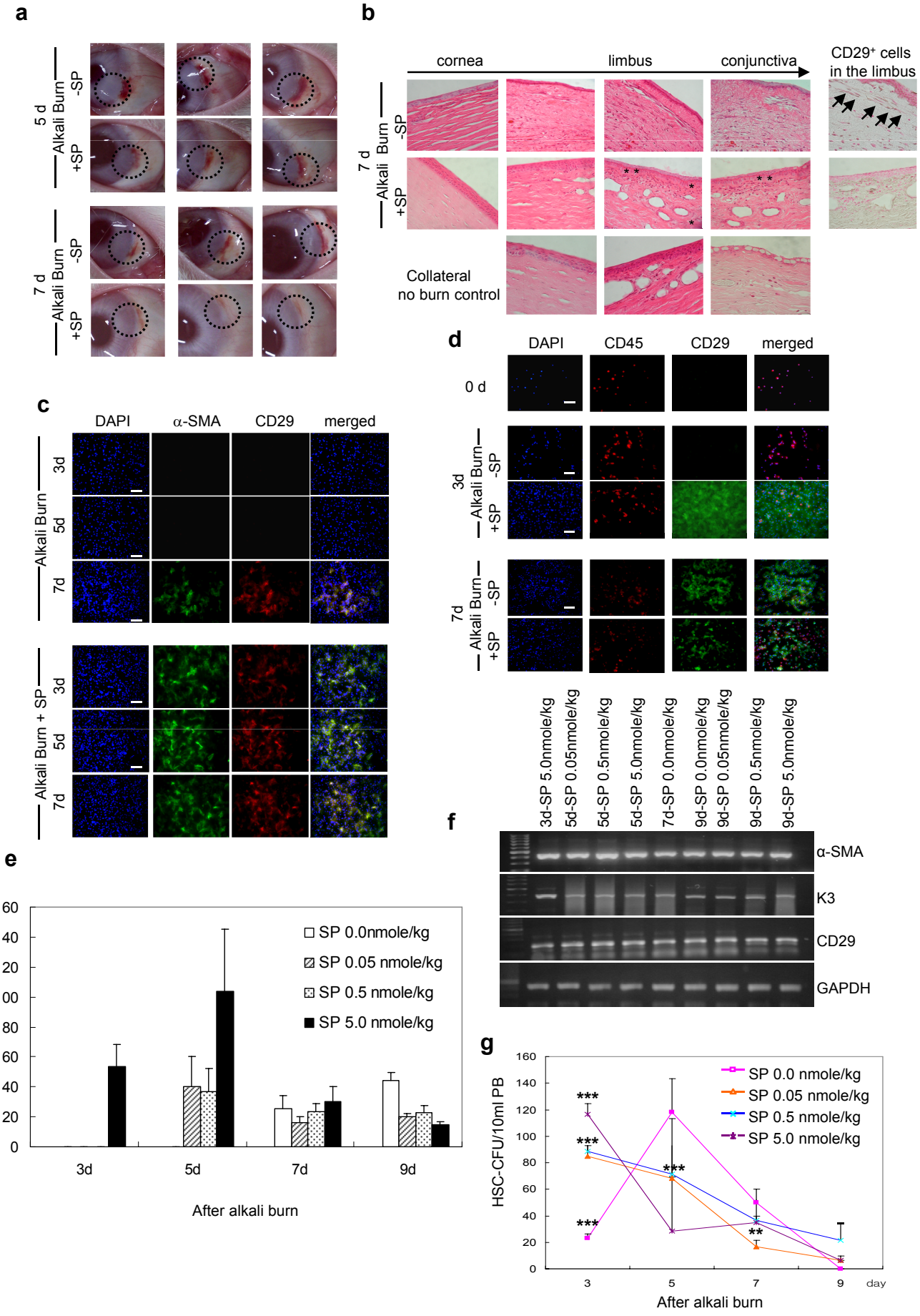

Figure 4

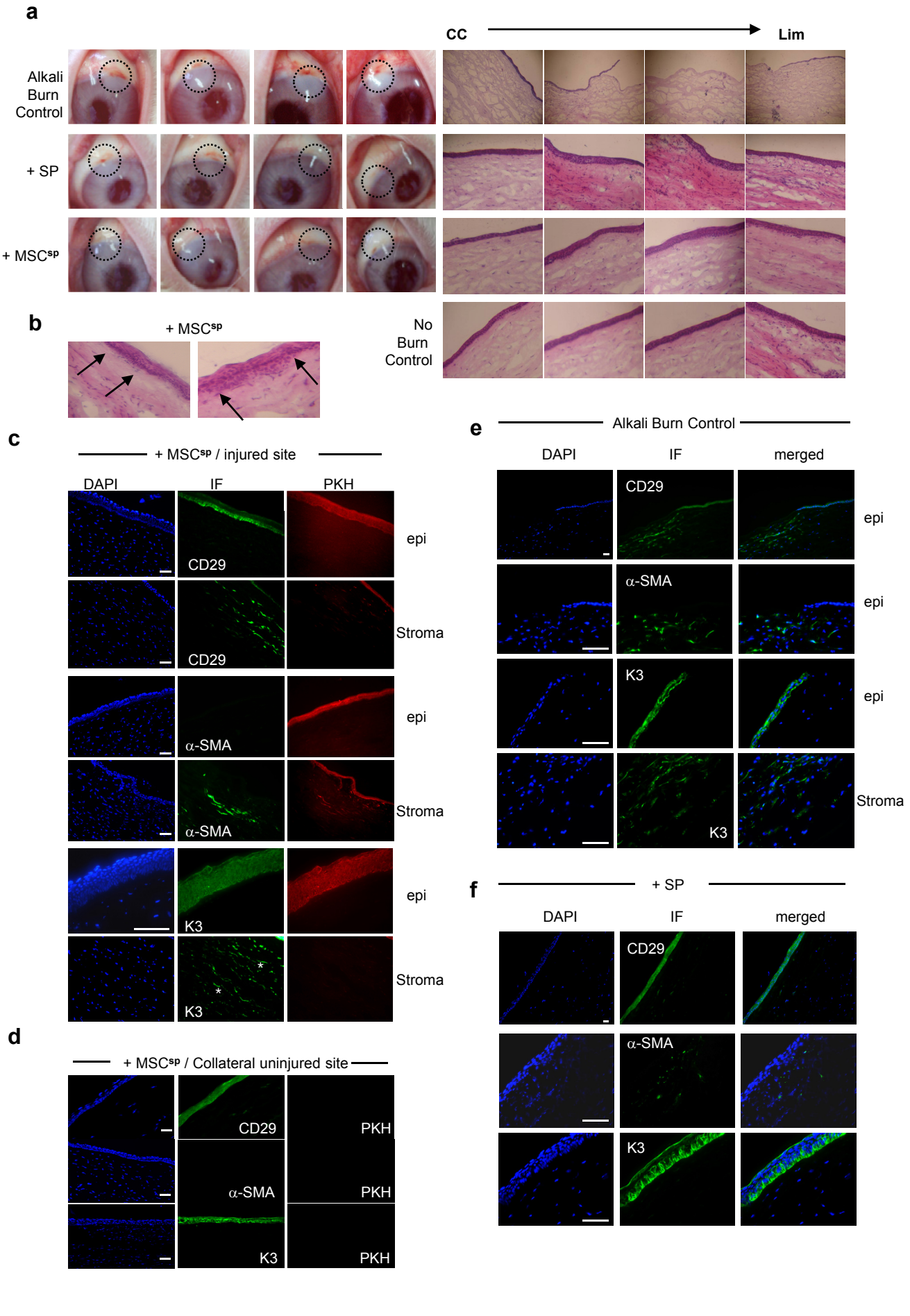

Figure 5

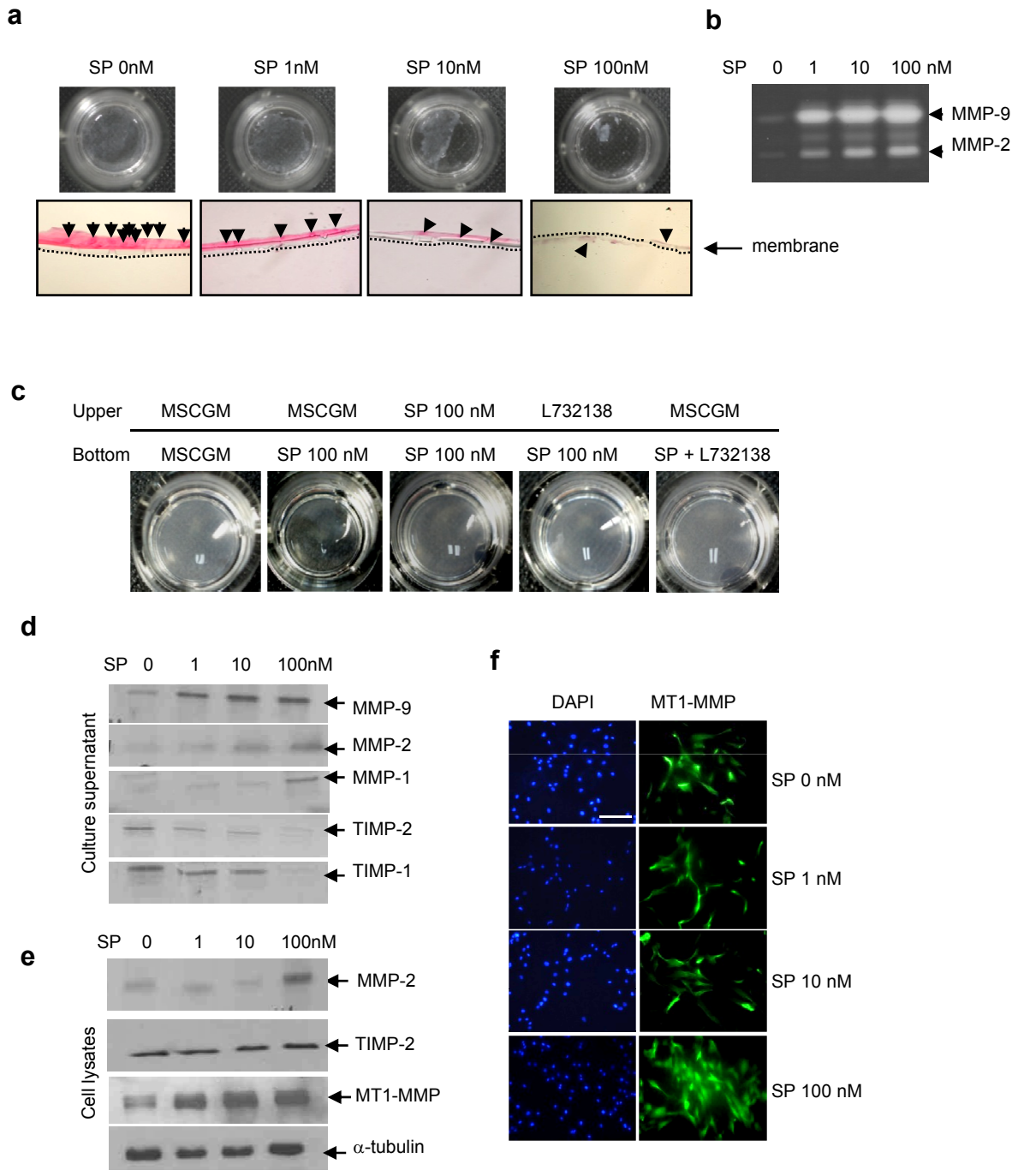

Figure 6